Theor Chem Acc (2009) 123:21–27
DOI 10.1007/s00214-009-0552-x

REGULAR ARTICLE

Static and dynamic properties of anionic intermolecular aggregates: the I^-–benzene–Ar_n case

M. Albertí · A. Aguilar · J. M. Lucas · F. Pirani

Received: 20 February 2009 / Accepted: 23 February 2009 / Published online: 19 March 2009

Abstract Molecular dynamics simulations on the I^-–benzene–Ar_n clusters have been carried out using an atom(ion)-bond model to describe the nonelectrostatic contribution to the total interaction. Results for I^-–benzene–Ar and I^-–benzene–Ar_n ($n = 3$, 18 and 25) are presented and some predicted properties are compared with those of the alkali cation–benzene clusters solvated by Ar atoms.

Keywords Molecular dynamics · Energy interaction · Clusters

1 Introduction

The investigation of structure and dynamics of weakly bound clusters, with a particular attention to their role in molecular recognition and selection [1–31] is an expanding subject of research for its interest in many fields. In particular, the interaction of ions with aromatic systems is relevant to various chemical processes occurring in biological systems [29, 30, 32]. These phenomena are typically governed by the combination of various components of the noncovalent intermolecular interaction, like electrostatic (of either attractive or repulsive nature), exchange or size (of repulsive nature), and induction and dispersion (of attractive nature). Unfortunately, it is quite difficult to accurately characterize the relative role played by the various components of noncovalent intermolecular interactions because, in general, they are much weaker than those leading to the usual chemical bonds and often they cannot be separable as the intermolecular distance decreases. The experience of some of us in modeling noncovalent interactions and the increasing research activity on molecular aggregates involving aromatic molecules, motivated the extension of an atom-bond type formulation of the atom–molecule interaction, originally developed for pure benzene (bz) rare-gas (Rg) systems [33, 34] to ion–bz and ion–bz–Rg_n aggregates. The most important characteristics of this model are the simplicity of the potential formulation and the closed relationship existing between the potential parameters and some basic physical properties of the few body fragments of the overall molecular aggregate. Moreover, the two-body atom-bond formulation of the interaction incorporates three-body effects in a natural way.

The potential model has been proved to be very useful in molecular dynamic simulations and it was first applied to investigate the alkali ion (M^+)–benzene systems (alone and solvated by rare gas atoms) and results show that the atom (ion)-bond formulation of the interaction is able to properly describe the potential energy surface (PES) and related steric and energetic features of the investigated systems. This has allowed, so far, to calculate both static and dynamic properties of the K^+–bz–Ar_n clusters [35], illustrating their specific steric biases with respect to those of bz–Ar_n [18, 19]. The model potential for the M^+–bz systems was tested against accurate ab initio calculations [36] and the comparison showed that the adopted representation is in general able to reproduce all the main features of the PES for these

Dedicated to Professor Santiago Olivella on the occasion of his 65th birthday and published as part of the Olivella Festschrift Issue.

M. Albertí (✉) · A. Aguilar · J. M. Lucas
IQTCUB, Departament de Química Física,
Universitat de Barcelona, Barcelona, Spain
e-mail: m.alberti@ub.edu

F. Pirani
Dipartimento di Chimica,
Universita di Perugia, Perugia, Italy

systems and the relative role of the leading interaction components. In particular, the agreement between the semiempirical model and ab initio results was found to be extremely good for the heavier metal cations (K^+, Rb^+ and Cs^+). Other systems containing alkali ions, rare gas atoms and benzene were investigated to analyze the size-specific interaction of alkali metal ions in the solvation of M^+–bz clusters by Ar atoms [37–39]. The same potential energy functions were used to study the effect of introducing Ar atoms in the sandwich bz–Rb^+–bz aggregate [40].

The chemistry of anions containing clusters is much less studied than that of cation clusters. This stems out of the intuitive mind that the charge distribution associated with the π electronic cloud of the aromatic ring stabilizes the cation–bz clusters while destabilizing the anion–bz ones. However, the design of new receptors stereoselectively binding anionic guests has fuelled a revisit to this topic [41–43]. Encouraged by the results obtained while investigating the alkali ion benzene systems, the model potential was applied to study the Cl^-–bz–Ar_n heterocluster [34] and their static and dynamic properties were compared with those of their K^+–bz–Ar_n homologues with n varying from 1 to 3. Here, we are interested to study the heavier I^-–bz–Ar_n and the effects produced when the number of atoms increases.

The present paper is organized as follows: In Sect. 2 the details of the potential energy function for I^-–bz–Ar_n clusters are presented. In Sect. 3, the behavior of I^-–bz–Ar, I^-–bz–Ar_3, I^-–bz–Ar_{18} and I^-–bz–Ar_{25} clusters is investigated by exploiting molecular dynamics simulations. Concluding remarks are given in Sect. 4.

2 Potential energy surface

As previously studied [35–39], the interaction potential is assumed to depend on the combination of electrostatic and nonelectrostatic contributions. The nonelectrostatic component, $V_{\rm nel}$, of the potential is constructed from ion-bond (6 I^-–CC and 6 I^-–CH), atom-bond (6 N Ar–CC and 6 N Ar–CH, N = number of Ar atoms) and atom (ion)-atom interactions as explained in Ref. [35]. Both, atom (ion)-bond and atom (ion)-atom interactions are described by means of an improved version of the Lennard Jones (ILJ) potential function [33], which removes most of inadequacies of the original version of the Lennard Jones model (LJ).

In the formulation of $V_{\rm nel}$, each atom(ion)-bond term is expressed as,

$$V(r,\alpha) = \varepsilon(\alpha)\left[\frac{m}{n(r,\alpha)-m}\left(\frac{r_0(\alpha)}{r}\right)^{n(r,\alpha)} - \frac{n(r,\alpha)}{n(r,\alpha)-m}\left(\frac{r_0(\alpha)}{r}\right)^{m}\right] \quad (1)$$

where r represents the distance between the atom and the center of the bond and α is the angle that the **r** vector forms with the bond. The m parameter is taken, respectively, equal to 6 and 4 for atom-bond and ion-bond interactions. The well depth ε and the equilibrium distance r_0 are modulated through simple trigonometric formula from the corresponding perpendicular and parallel components (see for instance Ref. [35]) to obtain $\varepsilon(\alpha)$ and $r_0(\alpha)$. The first term (positive) represents the size-repulsion contribution arising from each atom(ion)-bond pair, while the second one (negative) provides the corresponding dispersion and/or induction attraction effect.

The $n(r,\alpha)$ exponent, defining the falloff of the atom(ion)-bond repulsion is calculated as,

$$n(r,\alpha) = \beta + 4.0\left(\frac{r}{r_0(\alpha)}\right)^2 \quad (2)$$

where β, an adjustable parameter related to the hardness of the interacting partners, is taken, respectively, equal to 10 and 7 for Ar-bond and I^--bond interactions. Taking into account the higher polarizability of the I^- ion respect to that of Cl^-, the value of β has been lowered from 9 (the β value considered to describe the Cl^-–bz–Ar_n clusters) to 7.

The remaining parameters of the atom(ion)-bond interactions are given in Table 1.

By removing the angular dependence, Eqs. 1 and 2 are also used to describe both the I^-Ar and the Ar–Ar interactions, using, respectively, values of β equal to 7 and (as previously [35–37, 39]) 10. The remaining parameters for atom(ion)-atom interactions are given in Table 2.

All the parameters given in Tables 1 and 2, necessary to describe $V_{\rm nel}$ for the I^-–bz–Ar_n clusters, have been calculated using the charge and the polarizability of the related atomic species as well as polarizability and effective polarizability tensor components of aromatic C–C and C–H bonds [33, 44].

The electrostatic component of the interaction, $V_{\rm el}$, has been evaluated as in our previous studies of clusters containing ions and benzene, taking into account that $V_{\rm el}$ asymptotically must correspond to the ion quadrupole interaction (see for instance Ref. [35]). This leads to a charge of +0.09245 on each H atom and to two negative

Table 1 Perpendicular and parallel components of the deep well ($\varepsilon_\perp$, $\varepsilon_{||}$) and of the equilibrium distances ($r_{0\perp}$, $r_{0||}$) for the different atom(ion)-bond terms

Atom…bond	$\varepsilon_\perp$/meV	$\varepsilon_{||}$/meV	$r_{0\perp}$/Å	$r_{0||}$/Å
I^-…CC	13.76	52.96	4.166	4.380
I^-…CH	20.22	23.18	4.018	4.198
Ar…CC	3.895	4.910	3.879	4.189
Ar…CH	4.814	3.981	3.641	3.851

Table 2 Atom(ion)-atom interaction parameters

Atom…atom	ε/meV	r_0/Å	m
I^-…Ar	63.00	4.110	4
Ar…Ar	12.34	3.760	6

charges of −0.04623 separated by 1.905 Å on each C atom.

The total potential energy for I^-–bz–Ar_n is then formulated as,

$$V_{\text{total}} = V_{I^- - \text{bz}} + \sum_{i=1}^{n} V_{\text{Ar}_i - \text{bz}} + \sum_{i=1}^{n} V_{I^- - \text{Ar}_i} + \sum_{i=1}^{n-1} \sum_{j>i}^{n} V_{\text{Ar}_i - \text{Ar}_j} + V_{\text{el}} \quad (3)$$

where $V_{I^- - \text{bz}}$ and $V_{\text{Ar}_i - \text{bz}}$ denote, respectively, the contribution of the 12 ion-bond and the 12 atom-bond terms. Therefore, the first four terms define the nonelectrostatic contribution to total interaction.

In particular, the first term in Eq. 3 represents the interaction of the I^-–bz complex without electrostatic contribution. As found from ab initio calculations [45], our model predicts that the most stable structure of the I^-–bz complex is a planar C_{2v} structure in which I^- is hydrogen bonded to two adjacent CH groups (−272 meV) while the planar C_{2v} structure in which I^- approaches linearly to the CH bond is predicted to be less stable (−238 meV) than the bifurcated one. The bifurcated and linear forms of the I^-–bz complex are shown in Fig. 1. The distance from the anion to the center of mass of benzene is slightly shorter (5.19 Å) for the bifurcated structure than for the linear one (5.45 Å).

The second term of the equation is related to the interaction between Ar and benzene. The equilibrium structure for the dimer Ar–bz (−44.1 meV) is found at 3.53 Å from the center of mass of the aromatic ring when Ar approaches to benzene along the C_6 symmetry axis [33].

According to data in Table 3, the equilibrium energies for ion–Ar and Ar–Ar interactions (third and fourth terms in Eq. 3) are equal, respectively, to −63 and −12.34 meV.

These results indicate that, in general, the higher energy contribution in the I^-–bz–Ar_n aggregates with a few Ar atoms correspond to the I^-–bz interaction. However, as the number of Ar atoms increases, the other nonelectrostatic terms in Eq. 3 become higher.

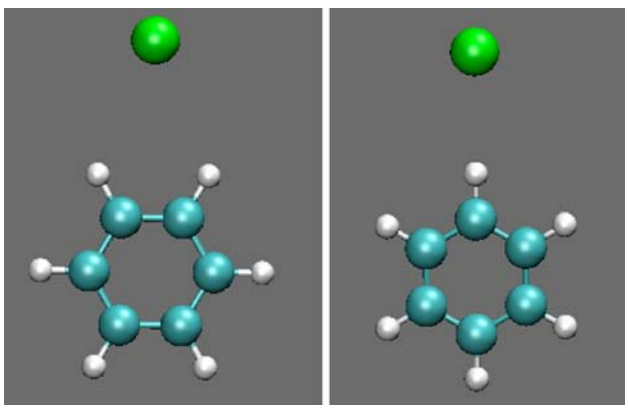

Fig. 1 Bifurcated (*left-hand side*) and linear (*rigth hand side*) forms of the I^-–bz complex

3 Molecular dynamic simulations

The study of the I^-–bz–Ar_n clusters has been carried out using the DL_POLY suite of programs (http://www.dl.ac.uk/TCSC/Software/DL_POLY). Dynamical simulations have been performed by considering a microcanonical ensemble (NVE) of atoms. The benzene molecule has been treated as a rigid body. Different total energy values (E_{total}) have been considered and the calculations have been carried out by looping over increasing values of E_{total}, which is calculated from the kinetic (E_k) and the potential (V_{total}) (see Eq. 3) energies. To reach the selected total energy value, an equilibration time has been considered when necessary. A time step of 1 fs has been used for all initial conditions. This time step is large enough to keep the fluctuations of E_{total} smaller than 10^{-5} meV. The simulation, at each new energy, has been initiated from the last configuration, velocities and forces of the last step of the previous run. The temperature T has been calculated from the relationship $T_i = 2E_k/k_B f$ (with k_B being the Boltzmann constant and f the number of degrees of freedom of the system) at each step and averaging all values. The total integration time for each simulation was set equal to 15 ns.

To help the rationalization of the results, the configuration energy (E_{cfg}) has been defined as the average of V_{total} over all the accessible configurations at the choosen total energy. The nonelectrostatic and electrostatic averages, contributing to E_{cfg} (E_{nel} and E_{el}), have also been considered together with the different components associated to the nonelectrostatic interaction arising from, ion–benzene ($E^-_{I-\text{bz}}$), Ar–benzene ($E_{\text{Ar-bz}}$), and the two body ion–Ar and Ar–Ar components (E_{two}).

The I^-–bz–Ar aggregate has only one stable energy with the anion placed on the plane of the aromatic ring. Because the different magnitude of the various energy components, the anion tends to stay very close to the equilibrium position (on the benzene plane) during the dynamic simulation, while the Ar atom is placed to interact with both benzene and anion, so that floating out of the

Table 3 Total configuration energy (E_{cfg}), ion–benzene (E^{-}_{I-bz}), Ar–benzene (E_{Ar-bz}), ion–Ar (E_{two}) and electrostatic (E_{el}) energies

E_{cfg}/meV	E^{-}_{I-bz}/meV	E_{Ar-bz}/meV	E_{two}/meV	E_{el}/meV	
−364.2	−178.1	−30.5	−62.8	−92.8	Equilibrium
−303.5	−163.4	−9.5	−48.1	−82.5	$T = 165$ K

benzene plane. Simulations at defined values of the total energy, chosen in the range from −363 to −267 meV, have been carried out and an increase of all energy contributions with E_{total} has been found. At low total energies, Ar oscillates near the equilibrium configuration and when the total energy increases, the atom can explore different zones of the PES and an increase of the different energy contributions, mainly that of E_{Ar-bz}, is observed. By further increasing E_{total}, when all accessible configurations of the cluster can be reached, the mean E_{Ar-bz} energy tends to remain constant. In this case, the Ar atom, flying far away from benzene, interacts only with the ion and, as a consequence, the probability of dissociation increases. At temperatures higher than 170 K the cluster can easily dissociate.

The dependence of the mean interaction energy between Ar and benzene (E_{Ar-bz}) as the temperature (or E_{total}) increases is shown, for the I^-–bz–Ar aggregate in Fig. 2 and in Table 3 the different energy contributions at the equilibrium geometry and at $T = 165$ K, are given. All energy results at $T = 165$ K correspond to the averaged values along the trajectory.

Both the nonelectrostatic (E^{-}_{I-bz}) and the electrostatic (E_{el}) energies, defining the total configuration energy for ion–bz ($E_{ion-bz} = E^{-}_{I-bz} + E_{el}$), provides larger contributions than E_{Ar-bz} and E_{two} (see Table 3). Accordingly, the ion typically tends to stay very close to the equilibrium position in the I^-–bz cluster being E_{ion-bz} at 165 K about 90% of the equilibrium value. Table 3 also shows that at

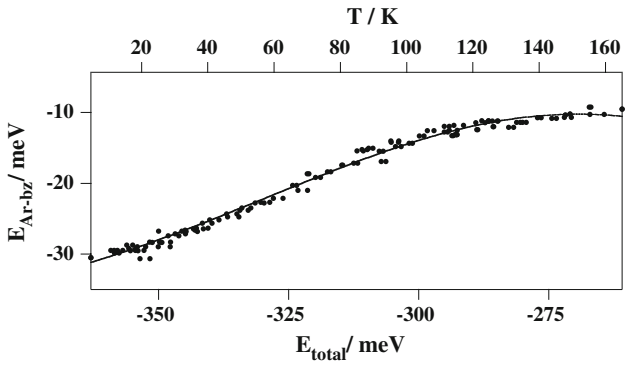

Fig. 2 Averaged Ar–bz energy contribution (E_{Ar-bz}) as a function of total energy (E_{total}) for the I^-–bz–Ar cluster

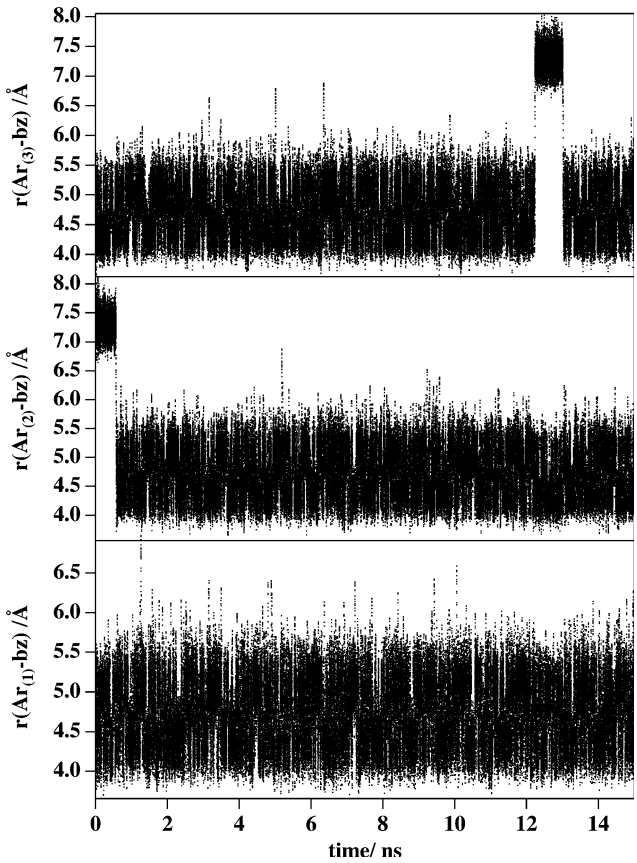

Fig. 3 Time evolution of the distances from the Ar atoms to the center of mass of benzene for the I^-–bz–Ar_3 cluster at 25 K of temperature

165 K, E_{cfg} accounts for about 83% of the equilibrium potential energy and that the higher percent of variation is for the Ar–bz contribution. This means that the Ar atom tends to be placed close to anion.

Aggregates with more than one Ar have more than one stable structure and isomerizations can be observed. For instance in the I^-–bz–Ar_3 cluster, the mobility of the Ar atoms contributes to frequent isomerizations, even at very low temperatures. These can be observed in Fig. 3, where the distances of the three Ar atoms to the center of mass (c.m) of benzene are represented along the simulation time at $T = 25$ K.

As can be seen in the figure, one of the Ar atoms (labeled as 1) vibrates without significant changes of the distance from benzene (bottom panel), so that its motion cannot be associated with isomerizations. The other two atoms, however, contribute to the cluster isomerization, one of them (labeled as 2) at the beginning of the simulation, leaving its position near the anion and approaching toward the benzene molecule (medium panel). The third Ar atom (labeled as 3), for about 1 ns approaches the anion to later return near benzene (top panel).

Taking into account, that the equilibrium distance between Ar and the benzene c.m is of 3.57 Å (for Ar atom placed on the C_6 axis of benzene) and of 5.15 and 5.52 Å (for on plane configurations of the Ar) [33], Fig. 3 seems to indicate that along the simulation, Ar atoms tend to occupy positions near the plane of the aromatic ring. Isomerizations at low temperatures are possible because several stable isomers, inter-connected through very low energy barriers, exist. The concerted movement of the atoms, searching the most favorable configurations, causes the increase of some energy contributions while other ones decrease. This can be observed in Fig. 4, where some results of a dynamical molecular simulation at 25 K are shown. The top panel of Fig. 4 shows the time evolution of the interaction energy between the three Ar atoms and the benzene molecule, while the bottom panel shows the time evolution of the overall two body (ion–Ar and Ar–Ar) energy contributions. As it can be seen in Fig. 4, the decrease of the Ar–bz energy (top panel) is accompanied by an increase of the two-body energy contribution (bottom panel). This was also observed for Cl^-–bz–Ar_2 [46] and confirms what is usually expected from a solvation process: the solvent molecules rearrange themselves in a way to compensate for the variation of the molecular geometries of the solute.

By further increasing the number of Ar atoms, these tend to be placed in the energetically most favorable positions, surrounding the I^-–bz cluster. When the number of Ar atoms is large enough it is better to study the cluster from the point of view of the I^-–bz solvation.

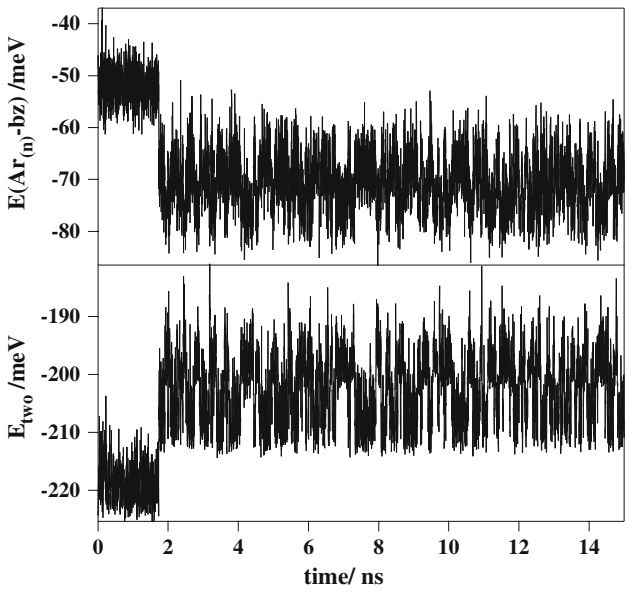

Fig. 4 Time evolution of the overall bz–Ar ($E_{Ar(n)–bz}$) and I^-Ar (E_{bnd}) energy contributions for the I^-–bz–Ar_3 cluster at 25 K of temperature

The gradual evolution from cluster rearrangement to solvation dynamics was studied for the alkali ions–bz clusters, solvated by Ar atoms [37, 38]. In the present study, the solvation of I^-–bz has been investigated considering 18 and 25 Ar atoms. These numbers are large enough to make evident some characteristics of solvation processes when studying the dynamics of the clusters.

Dynamical simulations of I^-–bz–Ar_{18} and I^-–bz–Ar_{25} show that the solvents prefer to occupy positions near I^-. This can be observed in Fig. 5 where the radial distribution function (rdf) of Ar atoms around I^- shows a high peak placed at $r \approx 4.1$ Å. This value of r is very close to the equilibrium value of 4.11 Å for the Ar–I^- interaction (see Table 2).

Figure 6 shows snapshots of the I^-–bz–Ar_{18} initial and final configurations (left-hand side and medium-hand side panels, respectively) and of the final configuration for I^-–bz–Ar_{25} (right-hand side panel). The comparison of initial and final configurations for I^-–bz–Ar_{18} suggests that Ar atoms flew away from benzene solvate the anion. Only when the number of atoms is further increased (I^-–bz–Ar_{25}), some of them solvate the benzene molecule (right-hand side panel).

The $E_{ion–bz}$ energy values, as can be expected, are the same for both clusters ($n = 18$ and 25), while a decrease of 332 meV for E_{two} and a decrease of 146 meV for $E_{Ar–bz}$ have been obtained when going from I^-–bz–Ar_{18} to I^-–bz–Ar_{25}. Despite the higher decrease in E_{two}, it must be taken into account that the number of two body terms for I^-–bz–Ar_{25} increase by 154 with respect to those for I^-–bz–Ar_{18}, while the Ar–bz interactions for I^-–bz–Ar_{25} increases only by 8 with respect to those for I^-–bz–Ar_{18}.

Significant differences have been found between the dynamics of Ar solvated alkali cation (M^+) [35–38] and I^-–bz clusters. These differences can then be explained from the magnitude of the various components of the interaction and from the different topology of the PES for cationic and anionic clusters. On one hand, both M^+–bz

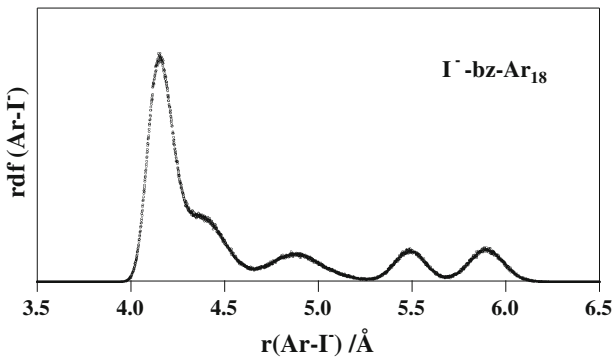

Fig. 5 Radial distribution function (*rdf*) of Ar atoms around I^- at 25 K for the I^-–bz–Ar_{18} cluster

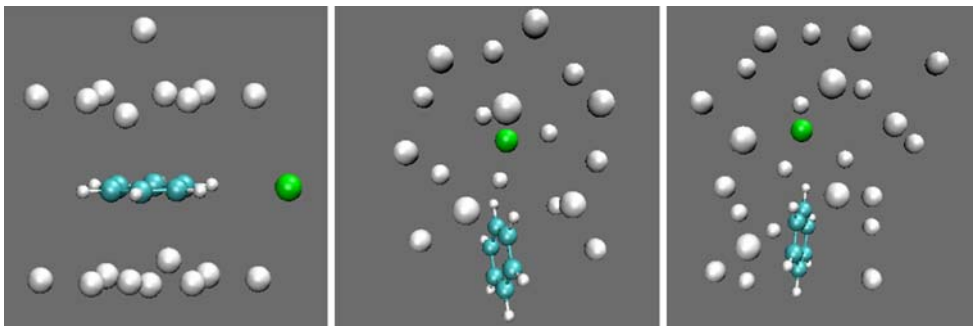

Fig. 6 *Left* and *medium side hand* Initial and final structures for the the I^-–bz–Ar_{18} cluster, respectively. *Right side hand* final structure for the the I^-–bz–Ar_{18} cluster

and I^-–bz clusters, because the magnitude of the interaction tend to remain in their equilibrium positions, while Ar atoms solvating the clusters tend to interact as much as possible with the ions (the bz–Ar interaction is weaker than the ion–bz ones). On the other hand, from a topological point of view, M^+–bz and I^-–bz are very different. For the M^+–bz clusters, the most stable configuration is found, when the cation approaches benzene perpendicularly to the aromatic ring, while the most stable configuration for I^-–bz has a six fold degenerate on-plane geometry. This originates only one isomer for I^-bz–Ar, while M^+–bz–Ar systems have two stable isomers, one of them with the Ar atom placed on the same side of the aromatic ring as the cation and the other with the cation and the atom placed on opposite sides of the benzene plane. Because of these differences, the Ar atoms solvating M^+–bz tend to move around the C_6 axis at distances close to r_0, the potential parameter of the M^+–Ar interaction. Thus, the Ar atoms placed near the cation are stabilized by both, the benzene molecule and the cation. On the contrary, the Ar atoms solvating I^-–bz around the anion interacts at a lower level with benzene tending to left bore the benzene when the total number of Ar atoms is not large enough.

4 Conclusions

The dynamics of some I^-bz–Ar_n clusters have been investigated from molecular dynamics simulations. The total potential energy function has been constructed by means of two-body, three-body (atom-bond) and electrostatic interactions. The use of Eq. 1, whose effectiveness has been recently provided by an extensive analysis of high resolution scattering experiments [47], permits to represent in a compact form the resulting of size repulsion and dispersion/induction attraction components.

In particular, the model is able to describe the key differences between M^+–bz and I^-–bz clusters, which show very different equilibrium structures. As previously was done for cation–bz systems [36], accurate ab initio calculations are in progress also on negative ion–bz systems to better assess the change of the relative role of the various interaction components with relative orientation and separation of involved partners and then to extend the model to more complex cases.

The potential energy function here adopted, very useful in molecular dynamic simulations, allows to describe steric and energetic properties of heteroclusters with relatively small computational effort.

The evolution of the different energy components has been analyzed for the I^-–bz–Ar cluster when increasing total energy. It has been found that the Ar atom prefers to be placed near the anion and that at temperatures higher than about 165 K, the cluster tends to dissociate in I^-–bz +Ar.

The addition of a small number of Ar atoms has been investigated for the I^-–bz–Ar_3 aggregate. Because the existence of several stable configurations, isomerization processes take place with a high probability even at low temperatures. The preferred configurations for I^-–bz–Ar_3 are those for which the Ar atoms are close to the anion.

The dynamics of I^-–bz–Ar_{18} and I^-–bz–Ar_{25} have been studied from the solvation of the I^-–bz cluster by Ar atoms. Results show the differences in the solvation process for I^-–bz with respect to that was observed for alkali ions–benzene. Moreover, results show that the Ar atoms tend preferably to occupy positions close to the anion.

Acknowledgments This paper is dedicated to Prof. Santiago Olivella, a good friend and better researcher, in appreciation of his contributions to theoretical chemistry. M. Albertí, A. Aguilar and J.M. Lucas acknowledge financial support from the Ministerio de Educación y Ciencia (Spain, Project CTQ2007-61109) and the Generalitat de Catalunya-DURSI (Project 2005 PEIR 0051/69). Also thanks are due to the Centre de Supercomputació de Catalunya CESCA-C4 and Fundació Catalana per a la Recerca for the allocated supercomputing time. F. Pirani acknowledges financial support from the Italian Ministry of University and Research (MIUR, PRIN 2005 Contracts No. 2004033958 and 2005033911_001).

References

1. Müller-Dethelfs K, Hobza P (2000) Chem Rev 100:143. doi: 10.1021/cr9900331

2. Alonso JL, Antolínez S, Bianco S, Lesarri A, López JC, Caminati W (2004) J Am Chem Soc 126:3244. doi:10.1021/ja038696u
3. Aquilanti V, Cornicchi E, Moix Teixidor M, Saendig N, Pirani F, Cappelletti D (2005) Angew Chem Int Ed 44:2336. doi:10.1002/anie.200462704
4. Dykstra CE, Lisy JM (2000) J Mol Struct Theochem 500:375. doi:10.1016/S0166-1280(00)00388-2
5. Ondrechen MJ, Berkovitch-Yellin Z, Jortner J (1981) J Am Chem Soc 103:6586. doi:10.1021/ja00412a009
6. Fried LE, Mukamel S (1991) J Chem Phys 96:116. doi:10.1063/1.462501
7. Schmidt M, Le Calvè J, Mons M (1993) J Chem Phys 98:6102. doi:10.1063/1.464849 and references therein
8. Mons M, Courty A, Schmidt M, Le Calvè J, Piuzzi F, Dimicoli I (1997) J Chem Phys 106:1676. doi:10.1063/1.473321
9. Easter DC, Bailey L, Mellot J, Tirres M, Weiss T (1998) J Chem Phys 108:6135. doi:10.1063/1.476023
10. Schmidt M, Mons M, Le Calvè J (1991) Chem Phys Lett 177:371. doi:10.1016/0009-2614(91)85068-8
11. Brupbacher T, Makarewicz J, Bauder A (1994) J Chem Phys 101:9736. doi:10.1063/1.467939
12. Hobza P, Bludsky O, Selzle HL, Schlag EW (1996) Chem Phys Lett 250:402. doi:10.1016/0009-2614(96)00008-5
13. Lenzer T, Luther K (1996) J Chem Phys 105:10944. doi:10.1063/1.472864
14. Bernshtein V, Oref I (2000) J Chem Phys 112:686. doi:10.1063/1.480714
15. Vacek J, Konvicka K, Hobza P (1994) Chem Phys Lett 220:85. doi:10.1016/0009-2614(94)00136-7
16. Vacek J, Hobza P (1994) J Phys Chem 98:11034. doi:10.1021/j100094a009
17. Dullweber A, Hodges MP, Wales DJ (1997) J Chem Phys 106:1530. doi:10.1063/1.473301
18. Riganelli A, Memelli M, Laganà A (2002) Lect Notes Comput Sci 2331:926. doi:10.1007/3-540-47789-6_97
19. Zoppi A, Becucci M, Pietraperzia G, Castellucci E, Riganelli A, Albertí M, Memelli M, Laganà A (2003) In: Clustering properties of rare gas atoms on aromatic molecules, 16th international symposium on plasma chemistry, Taormina, Italy, June, pp 22–27
20. Koch H, Fernández B, Makariewicz J (1999) J Chem Phys 111:198. doi:10.1063/1.479266
21. Dougherty DA (1996) Science 271:163. doi:10.1126/science.271.5246.163
22. Ma JC, Dougherty DA (1997) Chem Rev 97:1303. doi:10.1021/cr9603744
23. Mecozzi S, West AP Jr, Dougherty DA (1966) In: Proceedings of the National Academy of Sciences, USA, vol 93. p 10566
24. Tsuzuki S, Yoshida M, Uchimaru T, Mikami M (2001) J Phys Chem A 105:769. doi:10.1021/jp003287v
25. Felder C, Jiang HL, Zhu WL, Chen KX, Silman I, Botti SA, Sussman JL (2001) J Phys Chem A 105:1326. doi:10.1021/jp002933n
26. Mecozzi S, West AP, Dougherty DA (1996) J Am Chem Soc 118:2307. doi:10.1021/ja9539608
27. Cubero E, Luque FJ, Orozco M (1998) In: Proceedings of the National Academy of Sciences USA, vol 95. p 5976
28. Caldwell JW, Kollman PA (1995) J Am Chem Soc 117:4177. doi:10.1021/ja00119a037
29. Cabarcos OM, Weinheimer CJ, Lisy JM (1998) J Chem Phys 108:5151. doi:10.1063/1.476310
30. Cabarcos OM, Weinheimer CJ, Lisy JM (1999) J Chem Phys 110:8429. doi:10.1063/1.478752
31. Nicholas JB, Hay BP, Dixon DA (1999) J Phys Chem A 103:1394. doi:10.1021/jp9837380
32. Jalbout AF, Adamowicz L (2002) J Chem Phys 116:9672. doi:10.1063/1.1476012
33. Pirani F, Albertí M, Castro A, Moix M, Cappelletti D (2004) Chem Phys Lett 394:37. doi:10.1016/j.cplett.2004.06.100
34. Albertí M, Castro A, Laganà A, Pirani F, Porrini M, Cappelletti D, Liuti G (2004) Chem Phys Lett 392:514. doi:10.1016/j.cplett.2004.05.035
35. Albertí M, Castro A, Laganà A, Moix M, Pirani F, Cappelletti D (2005) J Phys Chem A 109:2906. doi:10.1021/jp0450078
36. Albertí M, Aguilar A, Lucas JM, Pirani F, Cappelletti D, Coletti C, Re N (2006) J Phys Chem A 110:9002. doi:10.1021/jp062007u
37. Albertí M, Aguilar A, Lucas JM, Laganà A, Pirani F (2007) J Phys Chem A 111:1780. doi:10.1021/jp066928g
38. Huarte-Larrañaga F, Aguilar A, Lucas JM, Albertí M (2007) J Phys Chem A 111:8072. doi:10.1021/jp073063d
39. Albertí M, Aguilar A, Lucas JM, Cappelletti D, Laganà A, Pirani F (2006) Chem Phys 328:221. doi:10.1016/j.chemphys.2006.06.030
40. Albertí M, Pacifici L, Laganà A, Aguilar A (2006) Chem Phys 327:105. doi:10.1016/j.chemphys.2006.03.042
41. Garau C, Frontera A, Quiñonero D, Ballester P, Costa A, Deyà PM (2003) Chem Phys Chem 4:1344. doi:10.1002/cphc.200300886
42. Garau C, Quiñonero D, Frontera A, Costa A, Ballester P, Deyà PM (2003) Chem Phys Lett 370:7. doi:10.1016/S0009-2614(03)00020-4
43. Beer PD, Gale PA (2001) Angew Chem Int Ed 40:486. doi:10.1002/1521-3773(20010202)40:3<486::AID-ANIE486>3.0.CO;2-P
44. Pirani F, Cappelletti D, Liuti G (2001) Chem Phys Lett 350:286. doi:10.1016/S0009-2614(01)01297-0
45. Loh ZM, Wilson RL, Wild DA, Bieske EJ, Zehnacker A (2003) J Chem Phys 119:9559. doi:10.1063/1.1615519
46. Albertí M, Castro A, Laganà A, Moix M, Pirani F, Cappelletti D (2006) Eur Phys J D 38:185. doi:10.1140/epjd/e2005-00303-6
47. Pirani F, Brizi S, Roncaratti LF, Casavecchia P, Cappelletti D, Vecchiocattivi F (2008) Phys Chem Chem Phys 10:5489. doi:10.1039/b808524b